Transverse momentum distributions in the nonperturbative region

Sonny Mantry and Frank Petriello

Phys. Rev. D **84**, 014030 — Published 22 July 2011

DOI: 10.1103/PhysRevD.84.014030

ANL-HEP-PR-10-57

Transverse Momentum Distributions in the Non-Perturbative Region

Sonny Mantry[1,*] and Frank Petriello[2,3,†]

[1] *University of Wisconsin, Madison, WI, 53706*

[2] *High Energy Physics Division, Argonne National Laboratory, Argonne, IL 60439, USA*

[3] *Department of Physics & Astronomy, Northwestern University, Evanston, IL 60208, USA*

Abstract

We study the low transverse momentum (p_T) distribution of the Z-boson at hadron colliders for $p_T \sim \Lambda_{QCD}$ using a factorization and resummation formula derived in the Soft Collinear Effective Theory (SCET). In the region $p_T \sim \Lambda_{QCD}$, new non-perturbative effects arise that cannot be entirely captured by the standard parton distribution functions, and require an additional new non-perturbative transverse momentum function (TMF). The TMF is field-theoretically defined in SCET, fully gauge invariant, and captures the non-perturbative dynamics that affects the p_T-distribution in the region $p_T \sim \Lambda_{QCD}$. The TMF also reduces to the expected perturbative result in the region $p_T \gg \Lambda_{QCD}$. We develop phenomenological models for these TMFs in the non-perturbative region, and discuss in detail fits to Tevatron data in which both experimental and theoretical errors are carefully treated.

*mantry147@gmail.com

†f-petriello@northwestern.edu

I. INTRODUCTION

The description of the low transverse momentum (p_T) distribution of electroweak gauge bosons and the Higgs boson has been the subject of extensive study [1–16]. It plays an important role in the precision measurement of the W-boson mass and Higgs boson searches while providing an important test of perturbative Quantum Chromodynamics (QCD). In the region of low transverse momentum $p_T \ll M$, where M denotes the mass of the electroweak gauge or the Higgs boson, large logarithms of p_T/M spoil the perturbative expansion in the strong coupling and require resummation.

More recently, the low-p_T resummation was studied using a factorization theorem derived [17, 18] in the Soft-Collinear Effective Theory (SCET) [19–21]. The result derived using SCET can be written entirely in momentum space, avoiding issues arising with the impact-parameter space present in the standard approach. All objects in the factorization theorem have well-defined operator expressions. A detailed study of the region $\Lambda_{QCD} \ll p_T \ll M$ was performed for the production of Higgs and electroweak gauge bosons. In this region, the factorization theorem is given entirely in terms of perturbatively calculable functions and the standard initial state parton distribution functions (PDFs), and takes the schematic form

$$\frac{d^2\sigma}{dp_T^2\, dY} \;\sim\; H \otimes \mathcal{G} \otimes f \otimes f. \tag{1}$$

Convolutions between the various objects are denoted by the symbol $\otimes$, H denotes a hard function whose renormalization group (RG) evolution sums logarithms of p_T/M, $\mathcal{G}$ denotes a perturbative function at the p_T-scale and describes the emission of soft and collinear partons that recoil against the heavy boson, and $f \otimes f$ denotes the product of the initial state PDFs which are evaluated at the p_T-scale as determined by DGLAP evolution. Resummation of the large logarithms was performed at the next-to-leading log (NLL) accuracy in Ref. [18] using renormalization group (RG) evolution in the effective theory. The results for the Z-boson are in excellent agreement with Tevatron data collected by the CDF [22] and D0 [23] collaborations.

In this paper, we turn our focus to the region $p_T \sim \Lambda_{QCD} \ll M$ where new non-perturbative effects arise that cannot be captured entirely by the standard PDFs. The region $p_T \sim \Lambda_{QCD}$ is sensitive to the transverse momentum distributions of the partons in

the initial state hadrons and to transverse momentum emissions of order Λ_{QCD}. In this region, the factorization formula takes the schematic form

$$\frac{d^2\sigma}{dp_T^2\, dY} \sim H \otimes \mathcal{K}, \tag{2}$$

where the function $\mathcal{K}$ is evaluated at the scale $\mu_T \sim p_T \sim \Lambda_{QCD}$. The definition of $\mathcal{K}$ is given in Section III. It is a new non-perturbative function that cannot be described in terms of the standard PDFs alone. In order to facilitate a smooth transition between Eqs. (2) and (1) as one increases p_T from non-perturbative to larger perturbative values, it is useful to write $\mathcal{K}$ in the form

$$\mathcal{K} \sim \mathcal{G} \otimes f \otimes f, \tag{3}$$

which defines the new transverse momentum function (TMF) $\mathcal{G}$. For phenomenological purposes, the TMF is modeled in the non-perturbative-p_T region with the constraint that it reduce to the expected perturbative result in Eq. (1) in the high-p_T region. For this reason we use the same symbol $\mathcal{G}$ to denote the TMF over the entire p_T spectrum. The function $\mathcal{K}$, or equivalently the TMF $\mathcal{G}$, is universal and depends only on the hadronic initial state.

The region of $p_T \sim \Lambda_{QCD}$ has been studied extensively in the context of semi-inclusive deep-inelastic scattering (SIDIS) [24–28], and also within the Collins-Soper-Sterman (CSS) approach to resummation of low-p_T logarithms [29–33]. In SIDIS processes, transverse momentum dependent parton distribution functions (TMDPDFs) typically arise in order to describe the order Λ_{QCD} dynamics in the initial hadrons. The TMDPDFs are typically not gauge invariant under singular gauge transformations, and arriving at a gauge-invariant definition has been the subject of much research [24–28, 34–39]. In our formalism, it is instead $\mathcal{K}$ that is the fundamental non-perturbative object in the region $p_T \sim \Lambda_{QCD}$. It is fully gauge invariant [17]. We choose to write $\mathcal{K}$ in the form of Eq. (3), and view the TMF ($\mathcal{G}$) and the PDFs (f) as the fundamental objects of interest. Both of these are manifestly gauge invariant, and have a more intuitive and smoother connection with the form of the factorization theorem in the region $p_T \gg \Lambda_{QCD}$. Furthermore, our formalism uses a different approach compared to the TMDPDF formalism. In particular, instead of TMDPDFs, our factorization formula is in terms of Impact-parameter Beam Functions (iBFs) which correspond to unintegrated PDFs and are fully differential in the momentum coordinates. These iBFs are interesting objects in their own right and worth further study due to their implications for the non-perturbative structure of the nucleon and universality.

The goal of this manuscript is to develop initial models of the TMF that satisfy the following criteria: they reduce smoothly to the perturbative result as one increases p_T, and they preserve the RG running of $\mathcal{K}$ in order to cancel the running of the hard function, as required by the scale invariance of the cross section. We do so, and present numerical results for $p\bar{p}$ initial states by fitting to Tevatron data. The fit discussed here is the first to incorporate the theoretical errors arising from scale variation in determining the non-perturbative parameters; this source of uncertainty has been neglected in previous fits within the CSS formalism [29]. We find that the theoretical error is the single largest source of uncertainty entering our fit. A global fit to all available data and an analysis of fixed-target data in order to describe the pp initial state and test the universality of the TMF is reserved for future work.

The outline of our paper is as follows. In Section II, we review the factorization formulas for the perturbative p_T region derived in [17, 18] and briefly discuss the various pieces and notation. In Section III we present the factorization formula for the non-perturbative p_T-region and discuss the issues involved in developing a non-perturbative model. We give phenomenological models for the TMF $\mathcal{G}$ in the non-perturbative p_T region and show numerical results in Section IV. We conclude in Section V.

II. THE PERTURBATIVE $\mathbf{p_T}$ REGION

In this section we briefly review the basic elements of the factorization and resummation formula for the transverse momentum distribution of the Z-boson in the region $\Lambda_{QCD} \ll p_T \ll M$, as derived in Refs. [17, 18]. Although we focus on the Z-boson, the analysis is similar for any color-neutral heavy final state. The appropriate effective field theory for this observable is $\mathrm{SCET_{II}}$, which has both collinear and soft degrees of freedom that can recoil against the Z-boson with transverse momenta of order p_T. The collinear and soft degrees of freedom have momentum scalings

$$p_n \sim M(\eta^2, 1, \eta), \qquad p_{\bar{n}} \sim M(1, \eta^2, \eta), \qquad p_s \sim M(\eta, \eta, \eta), \qquad \eta \sim \frac{p_T}{M_Z}, \tag{4}$$

where we have used the notation $p = (n \cdot p, \bar{n} \cdot p, p_\perp)$ to denote the light-cone and transverse momentum components. The light-cone four-vectors are $n^\mu = (1, 0, 0, 1)$ and $\bar{n}^\mu = (1, 0, 0, -1)$. The $p_{n,\bar{n}}$ momenta denote collinear momenta with large components

along the n^μ and $\bar{n}^\mu$ directions respectively. The soft momenta are denoted by p_s. The transverse momentum distribution in the region $\Lambda_{QCD} \ll p_T \ll M$ is dominated by these collinear and soft modes radiated from the initial state partons. In $\mathrm{SCET_{II}}$, these emissions build up into collinear and soft Wilson lines that dress the Z-production current. The final factorization and resummation formula for the differential cross-section of the Z-boson as a function of its transverse momentum and rapidity (Y) is given by

$$\begin{aligned}\frac{d^2\sigma}{dp_T^2\, dY} &= \frac{\pi^2}{N_c^2}\int_0^1 dx_1 \int_0^1 dx_2 \int_{x_1}^1 \frac{dx_1'}{x_1'}\int_{x_2}^1 \frac{dx_2'}{x_2'} \\ &\times\ H_Z^q(x_1x_2Q^2,\mu_Q;\mu_T)\,\mathcal{G}^{qrs}(x_1,x_2,x_1',x_2',p_T,Y,\mu_T) f_r(x_1',\mu_T) f_s(x_2',\mu_T).\end{aligned} \tag{5}$$

The above formula involves a convolution of three types of objects: the hard function H_Z^q, the TMF $\mathcal{G}^{qrs}$, and the initial state PDFs $f_{r,s}$. The indices r, s run over the initial partons and the superscript q denotes the fact that the Z-boson production vertex involves a quark current. The hard function describes the physics of modes with virtuality $p^2 \sim M^2$ that are integrated out at the scale $\mu_Q \sim M$. The hard function is then evolved down to the scale $\mu_T \sim p_T$ via its renormalization group equations, summing large logarithms of order M/p_T in the process. The TMF function $\mathcal{G}^{qrs}$ lives at the $\mu_T \sim p_T$ scale and describes the physics of the soft and collinear emissions in a way that is consistent with the constraints imposed on the p_T and Y of the Z-boson. The initial state PDFs $f_{r,s}$ are evaluated at the μ_T scale after DGLAP evolution from the non-perturbative scale, summing logarithms of order Λ_{QCD}/p_T in the process.

The TMF function $\mathcal{G}^{qrs}$ has the form

$$\begin{aligned}\mathcal{G}^{qrs}(x_1,x_2,x_1',x_2',p_T,Y,\mu_T) &= \int \frac{d^2b_\perp}{(2\pi)^2} J_0\big[b_\perp p_T\big] \int dt_n^+ dt_{\bar{n}}^-\, \mathcal{I}_{n;qr}\Big(\frac{x_1}{x_1'},t_n^+,b_\perp,\mu_T\Big) \\ \times\ \mathcal{I}_{\bar{n};\bar{q}s}\Big(\frac{x_2}{x_2'},t_{\bar{n}}^-,b_\perp,\mu_T\Big)&\mathcal{S}_{qq}^{-1}\Big(x_1Q - e^Y\sqrt{\mathrm{p}_T^2+M^2} - \frac{t_{\bar{n}}^-}{x_2Q}, x_2Q - e^{-Y}\sqrt{\mathrm{p}_T^2+M^2} - \frac{t_n^+}{x_1Q}, b_\perp,\mu_T\Big),\end{aligned} \tag{6}$$

where the functions $\mathcal{I}_{n;qr}, \mathcal{I}_{\bar{n};\bar{q}s}$ correspond to collinear emissions in the n and $\bar{n}$ directions respectively and $\mathcal{S}$ correspond to soft emissions. The inverse soft function (iSF) $\mathcal{S}^{-1}$ arises due to zero-bin subtractions [17, 18, 40–43] necessary to avoid the problem of double-counting the soft region. The collinear function $\mathcal{I}_{n;qr}$ is defined through the matching of a nucleon matrix element called the impact-parameter beam function (iBF) $\tilde{B}_n^q$ onto the standard

PDFs as

$$\tilde{B}_n^q(x,t,b_\perp,\mu_T) \equiv \int_x^1 \frac{dz}{z}\, \mathcal{I}_{n;qr}(\frac{x}{z},t,b_\perp,\mu_T)\, f_r(z,\mu_T), \tag{7}$$

with an analogous equation for the $\bar{n}$-sector. For precise field-theoretic definitions of the iBFs, the iSF, and the hard-function H_Z^q we refer the reader to Refs. [17, 18]. Analogous nucleon beam functions [44–47] are known to appear in other collider processes. We note that this SCET formalism accomplishes the resummation of large logarithms differently than the traditional QCD approach. Logarithms of the matching-scale ratio $\ln(\mu_Q/\mu_T)$ that appear in the partonic cross section are resummed via the RG evolution of H_Q^Z. Upon identifying $\mu_Q \sim M$ and $\mu_T \sim p_T$, these become the standard small-p_T logarithms. Kinematic logarithms which directly have $\ln(M/p_T)$ appear after integration over the momentum fractions $x'_{1,2}$ in Eq. (5). It was shown in Ref. [18] that this formalism reproduces the correct logarithms upon expansion of the resummed result to the fixed order $\mathcal{O}(\alpha_s^2)$ given our current knowledge of $\mathcal{G}$ in perturbation theory.

We comment briefly on the recent work of Ref. [48] which also uses SCET to address p_T-resummation. We disagree with several aspects of their results. Their analysis is based on the claim that the emission of soft radiation with transverse momentum of order p_T does not affect the spectrum of the Z-boson. This is in contrast to our effective field theory (EFT) where both collinear and soft radiation, with transverse momentum of order p_T, play a dynamical role in determining the transverse momentum spectrum. It is well-known [19–21] that the emission of multiple collinear and soft partons from the initial-state collinear partons build into eikonal Wilson lines and is a leading order effect in SCET_{II}. Since Ref. [48] argues against the presence of effects from soft radiation, their factorization formula does not have the analogue of the iSF. In our formalism the combined RG running of the two iBFs and the iSF cancels the running of the hard function as required by RG invariance. The presence of the iSF, which itself has a non-zero anomalous dimension, plays a crucial role in achieving this RG invariance as was shown in Ref. [17]. Since Ref. [48] does not have the iSF they do not naturally achieve the required RG invariance. Instead, RG invariance is implemented by introducing a 'hidden' Q^2 dependence in their two nucleon beam functions, which are individually ill-defined. This is done at the expense of losing field-theoretic operator definitions for the objects in their formula. This hidden Q^2 dependence is argued to arise from a collinear anomaly due to the absence of soft modes. It is further stated that soft modes have a vanishing contribution if the collinear anomaly is properly

regularized. Since the presence of the collinear-anomaly already assumes the absence of soft modes, we do not find this argument compelling. All of these problems are avoided if one starts with the correct degrees of freedom and includes the effects of both collinear and soft radiation. SCET_{II} is known to be the appropriate EFT for this purpose.

III. THE NON-PERTURBATIVE $\mathbf{p_T}$ REGION

In the previous section we reviewed the factorization formula for the region $\Lambda_{QCD} \ll p_T \ll M$. We now consider the p_T distribution in the region where $p_T \sim \Lambda_{QCD}$. The factorization theorem is given by

$$\frac{d^2\sigma}{dp_T^2\, dY} = \frac{\pi^2}{N_c^2} \int_0^1 dx_1 \int_0^1 dx_2 H_Z^q(x_1 x_2 Q^2, \mu_Q; \mu_T)\, \mathcal{K}^q(x_1, x_2, p_T, Y, \mu_T), \tag{8}$$

where $\mathcal{K}^q$ is defined as

$$\begin{aligned}\mathcal{K}^q(x_1, x_2, p_T, Y, \mu_T) \equiv & \int dt_n^+ \int dt_{\bar{n}}^- \int \frac{d^2 b_\perp}{(2\pi)^2} J_0(b_\perp p_T) \tilde{B}_n^q(x_1, t_n^+, b_\perp, \mu_T) \tilde{B}_{\bar{n}}^{\bar{q}}(x_2, t_{\bar{n}}^-, b_\perp, \mu_T) \\ & \times \mathcal{S}_{qq}^{-1}(x_1 Q - e^Y \sqrt{p_T^2 + M^2} - \frac{t_{\bar{n}}^-}{x_2 Q}, x_2 Q - e^{-Y} \sqrt{p_T^2 + M^2} - \frac{t_n^+}{x_1 Q}, b_\perp, \mu_T).\end{aligned} \tag{9}$$

In this case, the iBFs ($\tilde{B}_{n,\bar{n}}^q$) and the iSF ($\mathcal{S}_{qq}^{-1}$) are evaluated at the scale $\mu_T \sim p_T \sim \Lambda_{QCD}$ with the hard function H_Z^q evolved via its RG equations down to this same scale. Since $\mu_T \sim \Lambda_{QCD}$, the iBFs and the iSF are non-perturbative. We note that the iBF depends both light-cone momentum components and on the transverse spatial coordinate $b_\perp$. The iBF thus corresponds to a fully unintegrated PDF which is more differential than the TMDPDF. The iBF can thus be a powerful probe of nucleon structure and can arise in other differential observables. This expression for $\mathcal{K}^q$ was already derived in Ref. [17, 18]. In that work we focused on the region $p_T \gg \Lambda_{QCD}$ so that the iBFs and iSF were perturbative and the iBFs were further matched onto PDFs. In this case, since $\mu_T \sim p_T \sim \Lambda_{QCD}$, the iBFs and iSF are non-perturbative. A perturbative matching onto PDFs is no longer valid and the final form of the factorization theorem is given by Eqs. (8) and (9). For phenomenological purposes, the non-perturbative function $\mathcal{K}^q$ must be modeled. When $p_T \gg \Lambda_{QCD}$, the scale $\mu_T \sim p_T$ is perturbative. $\mathcal{K}^q$ then becomes a perturbative object and the iBFs can be matched onto PDFs as in Eq. (7), leading to Eq. (5).

We model the function $\mathcal{K}^q$ by imposing two requirements. First, the model for $\mathcal{K}^q$ must preserve the correct RG evolution properties so that it cancels the running of the hard function H_Z^q, as required by the scale invariance of the cross section. Second, as one increases p_T from the non-perturbative region to higher perturbative values, Eq. (8) must reduce to Eq. (5). In order to smoothly transition between the non-perturbative and perturbative values of p_T, we write the the iBFs in Eq. (9) as in Eq. (7), even in the non-perturbative region where $\mu_T \sim p_T \sim \Lambda_{QCD}$. In this region, Eq. (7) is no longer a perturbative matching equation but instead defines a new non-perturbative function $\mathcal{I}_{n;qr}$. As one increases $\mu_T \sim p_T$ to perturbative values, the function $\mathcal{I}_{n;qr}$ corresponds to the perturbatively calculable coefficient in the matching of the iBF onto the PDF. Similar statements apply to the $\bar{n}$-sector iBF. With these conventions, one can write the function $\mathcal{K}^q$ as

$$\mathcal{K}^q(x_1, x_2, p_T, Y, \mu_T) \equiv \sum_{r,s} \int_{x_1}^1 \frac{dx_1'}{x_1'} \int_{x_2}^1 \frac{dx_2'}{x_2'} \mathcal{G}^{qrs}(x_1, x_2, x_1', x_2', p_T, Y, \mu_T) f_r(x_1', \mu_T) f_s(x_2', \mu_T), \tag{10}$$

for *all* values of p_T. For perturbative p_T-values, the quantity $\mathcal{G}^{qrs}$ is perturbative and identical to that given in Eq. (6). The expression in Eq. (8) then properly reduces to the factorization theorem of Eq. (5), valid in the region $\Lambda_{QCD} \ll p_T \ll M_Z$. For $\mu_T \sim p_T \sim \Lambda_{QCD}$, $\mathcal{G}^{qrs}$ is non-perturbative, as are all the quantities on the RHS of Eq. (6). In the non-perturbative-p_T region, $\mathcal{G}^{qrs}$ can be interpreted as the non-perturbative TMF controlling the dynamics of transverse momentum dynamics of order Λ_{QCD}. The modeling of the function $\mathcal{K}^q$ in this region is reduced to the modeling of the TMF $\mathcal{G}^{qrs}$.

We view Eq. (10) with $\mathcal{K}^q$ rewritten in terms of the standard initial state PDFs and a new TMF function $\mathcal{G}^{qrs}$ as more convenient than the form in Eq. (9). Both ways of writing $\mathcal{K}^q$ are equally valid. In Eq. (9), the iBFs might be associated with TMDPDFs in the language used for the study of SIDIS processes. These iBFs are invariant under covariant gauge transformations but are not in general invariant under singular gauge transformations. However, the full product of the two iBFs and iSF that define $\mathcal{K}^q$ is completely gauge invariant. For a more detailed discussion of this point we refer the reader to Ref. [17]. The form of $\mathcal{K}^q$ in Eq. (10) makes gauge invariance manifest. Since both $\mathcal{K}^q$ and the PDFs are gauge invariant, the TMF $\mathcal{G}^{qrs}$ is also gauge independent. In Eq. (7), the gauge dependence of the iBF $\tilde{B}_n^q$ under singular gauge transformations is isolated into the function $\mathcal{I}_{n;qr}$. This situation also applies to the $\bar{n}$-sector iBF. The gauge dependence of the iBFs then cancels

in the product that defines $\mathcal{G}^{qrs}$. In this way, the non-perturbative dynamics in the region $p_T \sim \Lambda_{QCD}$ is described in terms of gauge invariant initial state PDFs and the TMF.

IV. TMF MODELS AND NUMERICAL RESULTS

In this section we develop phenomenological models for the TMF function $\mathcal{G}^{qrs}$ in the non-perturbative region. We require that the model for $\mathcal{G}^{qrs}$ reduces to the perturbatively calculable result as one increases p_T. We write $\mathcal{G}^{qrs}$ in the form

$$\begin{aligned}\mathcal{G}^{qrs}(x_1, x_2, x_1', x_2', p_T, Y, \mu_T) \;&=\; \int_0^\infty dp_T'\, \mathcal{G}^{qrs}_{\text{part.}}(x_1, x_2, x_1', x_2', p_T\sqrt{1+(p_T'/p_T)^2}, Y, \mu_T) \\ &\times\; G_{mod}(p_T', a, b, \Lambda),\end{aligned} \tag{11}$$

which is a convolution of the partonic result for the TMF function $\mathcal{G}^{qrs}_{\text{part.}}$ with a model function G_{mod} [49–51]. This form is reminiscent of that used in the CSS approach, where the integrand of the Fourier transform is decomposed according to

$$W(b) = W(b_*)W^{NP}(b), \quad b_* = \frac{b}{\sqrt{1+(b/b_{max})^2}}. \tag{12}$$

$W(b)$ is the perturbative resummed contribution and W^{NP} denotes the non-perturbative contribution. b_{max} is a free parameter typically taken to be of order $1\,\text{GeV}^{-1}$.

We parametrize our non-perturbative contribution as

$$G_{mod}(p_T', a, b, \Lambda) \;=\; \frac{2^{3/2-a}}{\Lambda}\frac{1}{\Gamma(a-1/2)}\left(\frac{p_T'^2}{\Lambda^2}\right)^{a-1}\exp\Big[-\frac{p_T'^2}{2\Lambda^2}\Big], \tag{13}$$

which satisfies the normalization condition

$$\int_0^\infty dp_T'\, G_{mod}(p_T', a, b, \Lambda) \;=\; 1. \tag{14}$$

We note that this function is approximately Gaussian, with a width given by Λ and a peak position $p^2_{T,peak} = 2(a-1)\Lambda^2$. By changing a and Λ we can therefore control both the peak and width of the non-perturbative transverse momentum contribution. We will find later that both parameters are constrained by data. As a simple check of the flexibility of our functional form, we have also tried a three-parameter non-perturbative model given by

$$G_{mod}(p_T', a, b, \Lambda) \;=\; \frac{N}{\Lambda^2}\left(\frac{p_T'^2}{\Lambda^2}\right)^{a-1}\exp\Big[-\frac{(p_T'-b)^2}{2\Lambda^2}\Big], \tag{15}$$

where N is fixed by the normalization condition in Eq. (14). We found that the new parameter b was unconstrained by the fit, while the best-fit values for a and Λ were similar to the two-parameter result. This indicates that the form of Eq. (13) is sufficiently flexible to describe the considered data sets.

In principle, the model function G_{mod} can have flavor indices r, s. For the sake of simplicity we will work with a flavor-independent model function G_{mod}. Different choices of the parameters a, Λ correspond to different model choices for the non-perturbative TMF $\mathcal{G}^{qrs}$. The model function parameters are chosen such that G_{mod} will peak at $p'_T \sim \Lambda_{QCD}$ with an exponential fall off for larger values of p'_T. As a result, $\mathcal{G}^{qrs}$ in Eq. (11) receives sizeable contributions only from the region $p'_T \sim \Lambda_{QCD}$. Thus, in the region $p_T \gg \Lambda_{QCD}$ one can Taylor expand $\mathcal{G}^{qrs}_{part.}$ around the limit $p_T \gg p'_T \sim \Lambda_{QCD}$. When combined with Eq. (14) this gives

$$\mathcal{G}^{qrs}(x_1, x_2, x'_1, x'_2, p_T, Y, \mu_T)\Big|_{p_T \gg \Lambda_{QCD}} = \mathcal{G}^{qrs}_{\rm part.}(x_1, x_2, x'_1, x'_2, p_T, Y, \mu_T) + \mathcal{O}(\frac{\Lambda_{QCD}}{p_T}). \tag{16}$$

In the region of perturbative p_T, the function $\mathcal{G}^{qrs}$ properly reduces to its perturbative limit with all model dependence suppressed by powers of Λ_{QCD}/p_T. In this way, the model dependence is restricted to the non-perturbative region, as expected. The perturbative region of the p_T spectrum remains calculable in a model-independent way to leading order in Λ_{QCD}/p_T. One could consider more sophisticated model functions that contain x-dependence and that incorporate additional effects, but we restrict ourselves in this initial analysis to the form of Eq. (13).

The implementation of the model also requires care regarding the choice of the scale μ_T. In the perturbative p_T region, the scale $\mu_T \sim p_T$ is the appropriate choice. However, one cannot use $\mu_T \sim p_T$ when p_T is of order Λ_{QCD} or smaller. The RG equations for the evolution of the hard function $H^q_Z(x_1 x_2 Q^2, \mu_Q; \mu_T)$ become non-perturbative in this region, and $\mathcal{G}^{qrs}_{part.}$ in Eq. (11) becomes incalculable. A sensible choice for μ_T that can be applied in both the perturbative and non-perturbative p_T regions is

$$\mu_T^2 = \xi^2\, p_T^2 + p_{Tmin}^2, \tag{17}$$

where $p_{Tmin} \gtrsim 1$ GeV is a low, but still perturbative, scale and can be viewed as another parameter of the model. It is analogous to the parameter b_{max} that appears in the CSS

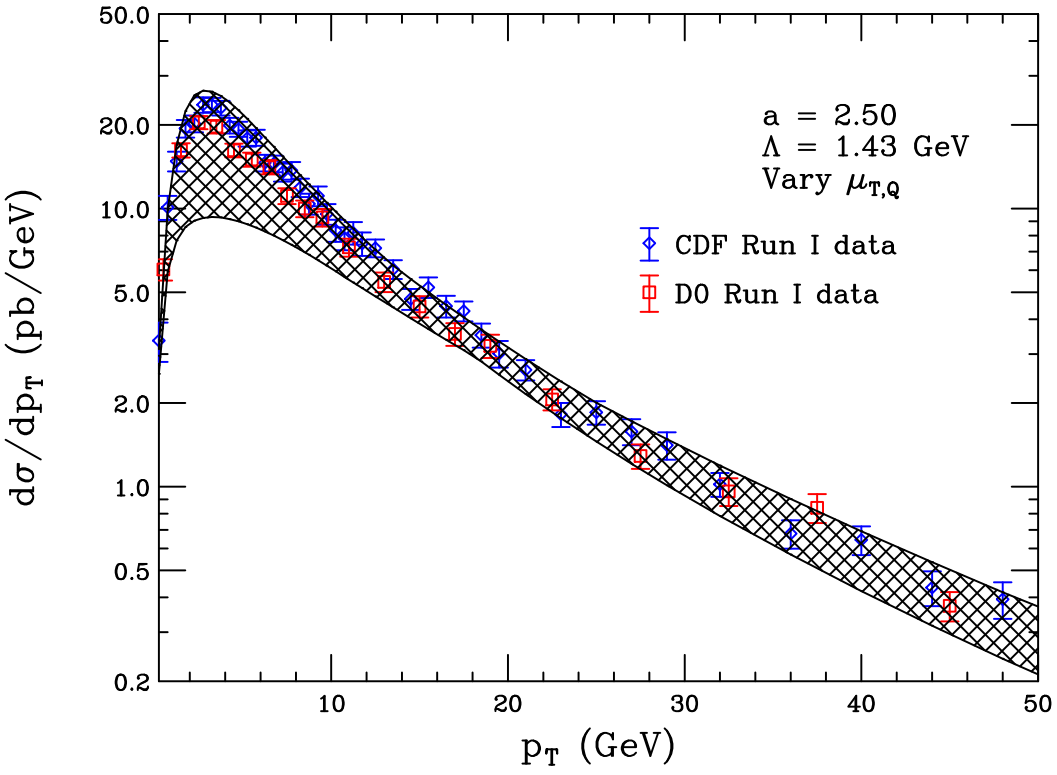

FIG. 1: The result for the p_T-spectrum of the Z-boson for the best fit parameter choices $a = 2.50, \Lambda = 1.43\,\text{GeV}$. We have varied $\mu_{T,Q}$ within the range set by Eq. (18). The data points were collected by the CDF and D0 collaborations [22, 23].

approach to transverse momentum resummation. ξ is a scale variation parameter we take to be $\mathcal{O}(1)$. The above choice of scale for μ_T has several useful properties. As $p_T \to 0$, the scale $\mu_T \to p_{Tmin}$ so that $\mathcal{G}^{qrs}_{part}$ in Eq. (11) is still evaluated at a perturbative scale. Similarly, the running of the hard function $H^q_Z(x_1 x_2 Q^2, \mu_Q; \mu_T)$ will freeze at the perturbative scale p_{Tmin} as $p_T \to 0$. For larger values of $p_T \gg p_{Tmin} \gtrsim 1$ GeV, $\mu_T \to \xi\, p_T$ so that the appropriate choice of $\mu_T \sim p_T$ in the perturbative region is recovered.

A. Details of the TMF fit

We now discuss in detail our fit of the TMF function $\mathcal{G}^{qrs}$ to Tevatron data for the Z-boson p_T spectrum. We perform a chi-squared fit of the parameters a and Λ in Eq.(13) against CDF and D0 data [22, 23]. Only data from p_T bins below 10 GeV is used. Transverse momenta above 10 GeV are completely insensitive to the values of the non-perturbative

parameters. We set $p_{T,min} = 2$ GeV in Eq. (17) for two primary reasons. First, this ensures that the scale μ_T at which the PDFs are evaluated always remains at or above the initial scale $Q_0 = 1$ GeV used in the MSTW fit [54], a criterion pointed out in previous work in the CSS approach [31]. Second, if $p_{T,min}$ varies within a specified range, the lowest value allowed will always be returned as the best-fit value, as this choice increases the scale-variation error and consequently reduces the chi-squared. A value of 2 GeV prevents the error defined by Eq. (17) from being so large as to remove sensitivity to different models in the low p_T region. Several sources of error enter the TMF fit. We handle them as discussed below.

- Theory error: We define our theoretical error by varying the scales μ_T and μ_Q freely in the ranges

$$\begin{aligned} \mu_T^2 &= \xi_T^2\, p_T^2 + p_{Tmin}^2, \\ \mu_Q^2 &= -M_Z^2\, \xi_Q^2, \end{aligned} \tag{18}$$

  with $\xi_{T,Q}$ separately varied through the region $1/2 < \xi_{T,Q} < 2$. The central value for the hard matching scale μ_Q is chosen according the the arguments presented in Ref. [52, 53]. A central value and symmetric error are defined for each bin by taking the envelope of values arising from the scale variation and computing the midpoint. The variations of ξ_T and ξ_Q are correlated across all p_T bins. The theoretical error is the largest source of uncertainty, with the diagonal entries of the error matrix reaching nearly 50% for $p_T \approx 3-4$ GeV. We have considered uncertainties arising from imprecise knowledge of parton distribution functions, and have found them to be smaller than the scale error.

- Luminosity error: The luminosity measurement during Run I of the Tevatron was determined from a combination of the total inelastic cross sections determined by CDF and D0, together with measurements from other experiments such as E710 and E811 [55, 56]. This leads to a division of the luminosity error into a component 100% correlated between the two experiments, and an uncorrelated component. A simple approximation valid for our purposes can be adopted [57]: assign a 4% error component which is 100% correlated across all bins and all experiments, and add another 4% component uncorrelated between CDF and D0. This approximates the luminosity error to an accuracy of 10%, sufficient for our purposes.

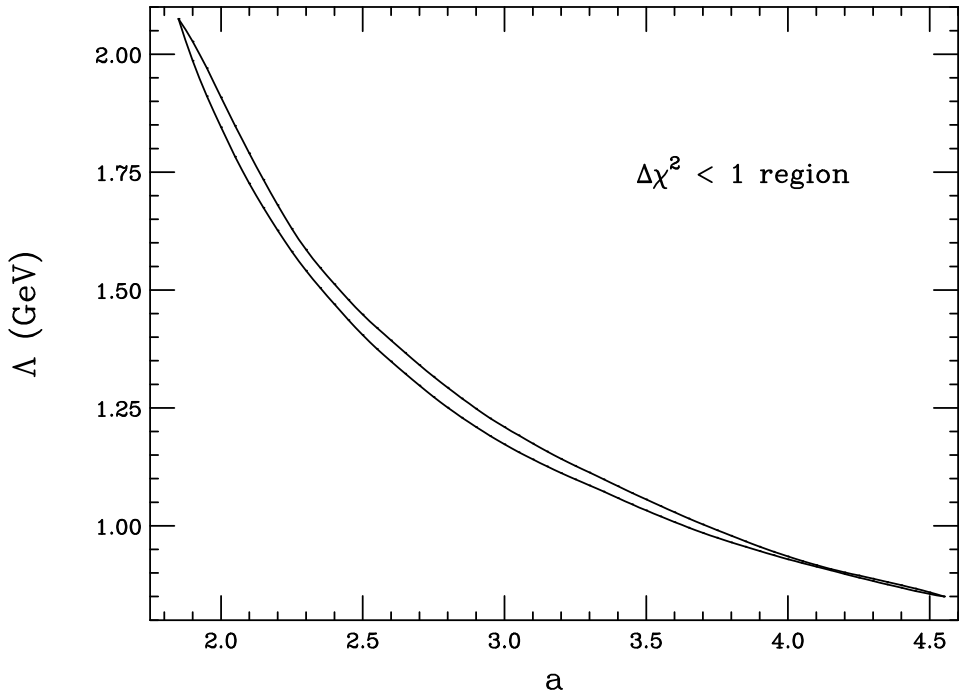

FIG. 2: The $\Delta\chi^2 < 1$ region for the parameters a, Λ.

- Experimental statistics and other systematics: Both CDF and D0 quote an error on each p_T bin of their data set, which includes both the statistical error and various systematic effects such as uncertainties due to detector response [22, 23]. The magnitude of this error varies between approximately $5 - 15\%$ as a function of p_T. The correlation matrix for these errors is not given. However, since this error is sub-dominant to the theory error and since its statistical component is significant, we treat it as uncorrelated across all bins for simplicity.

With these preliminaries dispensed with, we can proceed to discuss the results of our fit for the parameters a and Λ. We find the best-fit values for the parameters $a = 2.50$ and $\Lambda = 1.43$ GeV, with a goodness-of-fit measure $\chi^2_{min}/d.o.f. \approx 0.6$. The result for these best fit values, together with the uncertainty arising from the scale variation defined in Eq. (18), is shown in Fig. 1 along with the CDF and D0 data points. Fig. 1 shows that the TMF model is flexible enough to give a good description of data in the region $p_T < 1$ GeV where non-perturbative transverse momentum dynamics becomes important. At the same time, a good description of the data is also achieved for larger perturbative values of p_T where the result is given in terms of a perturbatively calculable TMF function. It is clear that the

uncertainty arising from scale variation is large in the low p_T region. A further reduction of this error requires resummation to next-to-next-to-leading logarithmic accuracy, which is currently underway within our approach [58].

We can define the standard $1-\sigma$ errors for the parameters a, Λ by searching for values of these quantities for which $\Delta\chi^2(a,\Lambda) \equiv \chi^2(a,\Lambda) - \chi^2_{min} < 1$. Doing so, we find

$$a = 2.50^{+2.05}_{-0.65}, \qquad \Lambda = 1.43^{+0.67}_{-0.58}\,\mathrm{GeV}. \tag{19}$$

While Λ has an approximately symmetric error, a possesses a tail toward large values, indicating that the χ^2 function deviates from a parabolic form. Pragmatic methods for the treatment of such errors has been discussed [59], and can be implemented in future studies if this error must be combined with others. The parameters a and Λ are highly anti-correlated, as shown in Fig. 2. We note that the allowed ranges of a, Λ are larger than the allowed regions for the analogous parameters in the CSS approach [29]. This is due in part to the neglect of uncertainty arising from scale variation in those previous fits; we find that this effect significantly hinders the extraction of the non-perturbative parameters.

The model dependence introduced by G_{mod} turns off in the region $p_T \gg \Lambda_{QCD}$, as expected. This is further illustrated in Fig. 3 where we show the predictions of all models passing the $\Delta\chi^2 < 1$ constraint for the two scale choices $\xi_T = \xi_Q = 2$ and $\xi_T = \xi_Q = 1$. We see in Fig. 3 that while the different parameter choices affect the p_T-distribution in the non-perturbative region, there is little effect in the region $p_T \gg \Lambda_{QCD}$. This is a reflection of Eq. (16) which shows that for $p_T \gg \Lambda_{QCD}$ the model dependence is power suppressed and the TMF function reduces to the expected partonic result.

Before concluding we comment briefly on the universality of G_{mod}. We have neglected the possible flavor dependence of this function in our fit, indicating that we expect the non-perturbative dynamics of the valence up and down quarks that dominate Z-boson production at the Tevatron to be the same. However, it remains to be seen whether the valence-sea scattering which occurs in pp collisions can be described by the same G_{mod}. For this reason we refrain from making predictions for LHC production until this universality is tested by a detailed fit to the available data. We note that W^{NP} in the CSS approach has been found to satisfy the universality assumption [31].

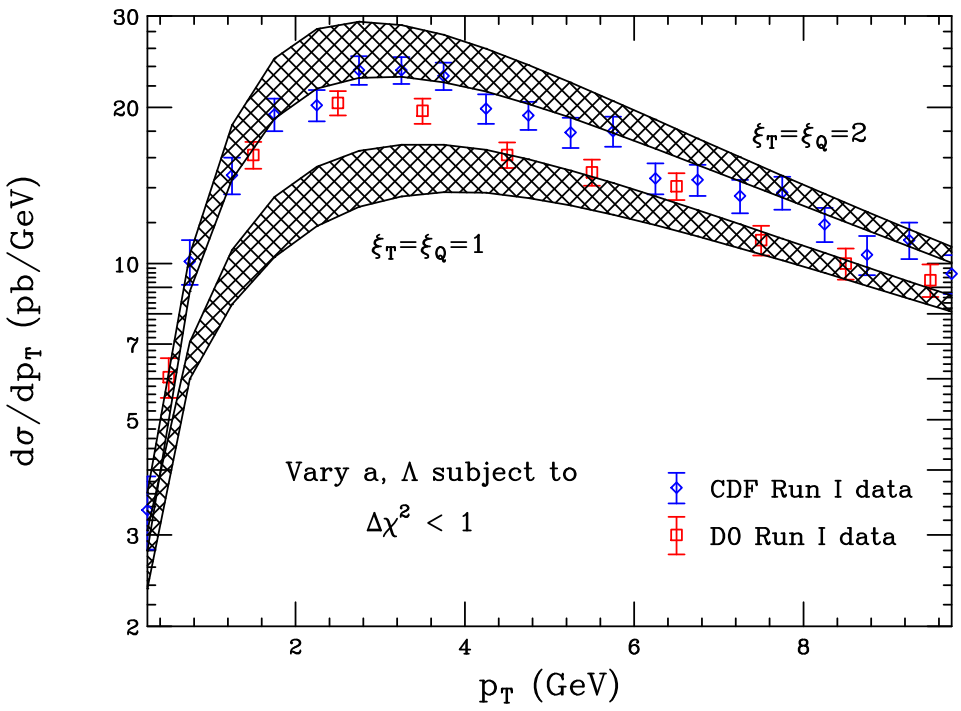

FIG. 3: The result of varying the model parameters a and Λ within the region defined by $\Delta\chi^2 < 1$. We have made the two scale choices $\xi_T = \xi_Q = 2$ and $\xi_T = \xi_Q = 1$ for illustration. We see that the variation of the model parameters affects primarily the very low p_T region and has a small effect in the region $p_T \gg \Lambda_{QCD}$. The data points are from the CDF and D0 collaborations [22, 23].

V. CONCLUSIONS

In this manuscript we have performed an initial analysis of the Z-boson transverse momentum distribution in the region $p_T \sim \Lambda_{QCD}$ using a factorization and resummation theorem derived in SCET. Combined with our previous work [17, 18] which focused on the region $\Lambda_{QCD} \ll p_T \ll M$, a description of the entire p_T-spectrum is now achieved in the framework of SCET. This formalism is free of the Landau poles that arise in the traditional approach to low-p_T resummation in impact-parameter space, and are therefore independent of ambiguities and numerical difficulties which arise when transforming back to momentum space. In the region where $p_T \sim \Lambda_{QCD}$, the transverse momentum spectrum is affected by new non-perturbative effects that cannot be described by the standard PDFs alone. A new transverse momentum function (TMF), fully gauge invariant and defined in SCET, arises in addition to the standard PDFs. The TMF captures the non-perturbative dynamics associated with the initial state transverse momentum distributions and with final-state emissions

having transverse momenta of order Λ_{QCD}. We have devised phenomenological models for the TMFs in the region $p_T \sim \Lambda_{QCD}$. These models are such that the TMF reduces to the expected perturbative result when $p_T \gg \Lambda_{QCD}$. This allows for a smooth transition between the non-perturbative and perturbative values of p_T. The TMF models also have the correct renormalization group evolution properties built in. We have described in detail a fit of the TMF model to Tevatron data. Both experimental errors and theoretical errors arising from scale variation are carefully treated. The results of the fit for the TMF function give a good description of the CDF and D0 data over the entire p_T spectrum.

The work presented here is simply the first step in understanding the non-perturbative transverse momentum region within SCET. A more global analysis of the available data is left to future work, as is the modeling of the TMF for pp initial states. In principle, the TMF is different for pp and $p\bar{p}$ initial states. The universality of this function remains to be studied. These questions must be addressed to present predictions for the p_T distribution at the LHC. We look forward to these future investigations.

Acknowledgments

We thank H. Schellman and M. Schmitt for helpful discussions. This work is supported in part by the U.S. Department of Energy, Division of High Energy Physics, under contract DE-AC02-06CH11357 and the grants DE-FG02-95ER40896 and DE-FG02-08ER4153, and by Northwestern University.

---

[1] Y. L. Dokshitzer, D. Diakonov, and S. I. Troian, Phys. Lett. **B79**, 269 (1978).

[2] G. Parisi and R. Petronzio, Nucl. Phys. **B154**, 427 (1979).

[3] G. Curci, M. Greco, and Y. Srivastava, Nucl. Phys. **B159**, 451 (1979).

[4] J. C. Collins and D. E. Soper, Nucl. Phys. **B193**, 381 (1981).

[5] J. C. Collins, D. E. Soper, and G. Sterman, Nucl. Phys. **B250**, 199 (1985).

[6] R. P. Kauffman, Phys. Rev. **D44**, 1415 (1991).

[7] C. P. Yuan, Phys. Lett. **B283**, 395 (1992).

[8] R. K. Ellis and S. Veseli, Nucl. Phys. **B511**, 649 (1998), hep-ph/9706526.

[9] A. Kulesza, G. Sterman, and W. Vogelsang, Phys. Rev. **D66**, 014011 (2002), hep-ph/0202251.

[10] E. L. Berger and J.-w. Qiu, Phys. Rev. **D67**, 034026 (2003), hep-ph/0210135.

[11] G. Bozzi, S. Catani, D. de Florian, and M. Grazzini, Phys. Lett. **B564**, 65 (2003), hep-ph/0302104.

[12] A. Kulesza, G. F. Sterman, and W. Vogelsang, Phys. Rev. **D69**, 014012 (2004), hep-ph/0309264.

[13] G. Bozzi, S. Catani, D. de Florian, and M. Grazzini, Nucl. Phys. **B737**, 73 (2006), hep-ph/0508068.

[14] G. Bozzi, S. Catani, G. Ferrera, D. de Florian, and M. Grazzini, (2010), 1007.2351.

[15] Y. Gao, C. S. Li, and J. J. Liu, Phys. Rev. **D72**, 114020 (2005), hep-ph/0501229.

[16] A. Idilbi, X.-d. Ji, and F. Yuan, Phys. Lett. **B625**, 253 (2005), hep-ph/0507196.

[17] S. Mantry and F. Petriello, Phys. Rev. **D81**, 093007 (2010), 0911.4135.

[18] S. Mantry and F. Petriello, (2010), 1007.3773.

[19] C. W. Bauer, S. Fleming, D. Pirjol, and I. W. Stewart, Phys. Rev. **D63**, 114020 (2001), hep-ph/0011336.

[20] C. W. Bauer, D. Pirjol, and I. W. Stewart, Phys. Rev. **D65**, 054022 (2002), hep-ph/0109045.

[21] C. W. Bauer, S. Fleming, D. Pirjol, I. Z. Rothstein, and I. W. Stewart, Phys. Rev. **D66**, 014017 (2002), hep-ph/0202088.

[22] CDF, A. A. Affolder *et al.*, Phys. Rev. Lett. **84**, 845 (2000), hep-ex/0001021.

[23] D0, B. Abbott *et al.*, Phys. Rev. Lett. **84**, 2792 (2000), hep-ex/9909020.

[24] J. C. Collins, Nucl. Phys. **B396**, 161 (1993), hep-ph/9208213.

[25] X.-d. Ji, J.-p. Ma, and F. Yuan, Phys. Rev. **D71**, 034005 (2005), hep-ph/0404183.

[26] I. O. Cherednikov and N. G. Stefanis, Phys. Rev. **D77**, 094001 (2008), 0710.1955.

[27] I. O. Cherednikov and N. G. Stefanis, Nucl. Phys. **B802**, 146 (2008), 0802.2821.

[28] I. O. Cherednikov and N. G. Stefanis, Phys. Rev. **D80**, 054008 (2009), 0904.2727.

[29] F. Landry, R. Brock, G. Ladinsky, and C. P. Yuan, Phys. Rev. **D63**, 013004 (2001), hep-ph/9905391.

[30] J.-w. Qiu and X.-f. Zhang, Phys. Rev. **D63**, 114011 (2001), hep-ph/0012348.

[31] A. V. Konychev and P. M. Nadolsky, Phys. Lett. **B633**, 710 (2006), hep-ph/0506225.

[32] F. A. Ceccopieri, Mod. Phys. Lett. **A24**, 3025-3032 (2009). [arXiv:0910.2934 [hep-ph]].

[33] R. Gastmans, S. L. Wu, T. T. Wu, Phys. Lett. **B693**, 452-455 (2010).

[34] X.-d. Ji and F. Yuan, Phys. Lett. **B543**, 66 (2002), hep-ph/0206057.

[35] J. C. Collins, F. Hautmann, Phys. Lett. **B472**, 129-134 (2000). [hep-ph/9908467].

[36] F. Hautmann, Phys. Lett. **B655**, 26-31 (2007). [hep-ph/0702196 [HEP-PH]].

[37] A. Idilbi and I. Scimemi, (2010), arXiv:1009.2776.

[38] A. Idilbi and A. Majumder, Phys. Rev. **D80**, 054022 (2009), 0808.1087.

[39] C. W. Bauer, B. O. Lange, and G. Ovanesyan, (2010), arXiv:1010.1027.

[40] A. V. Manohar and I. W. Stewart, Phys. Rev. **D76**, 074002 (2007), hep-ph/0605001.

[41] C. Lee and G. Sterman, Phys. Rev. **D75**, 014022 (2007), hep-ph/0611061.

[42] A. Idilbi and T. Mehen, Phys. Rev. **D75**, 114017 (2007), hep-ph/0702022.

[43] A. Idilbi and T. Mehen, Phys. Rev. **D76**, 094015 (2007), 0707.1101.

[44] S. Fleming, A. K. Leibovich, and T. Mehen, Phys. Rev. **D74**, 114004 (2006), hep-ph/0607121.

[45] I. W. Stewart, F. J. Tackmann, and W. J. Waalewijn, (2009), 0910.0467.

[46] I. W. Stewart, F. J. Tackmann, and W. J. Waalewijn, (2010), 1005.4060.

[47] I. W. Stewart, F. J. Tackmann, and W. J. Waalewijn, (2010), 1002.2213.

[48] T. Becher and M. Neubert, (2010), 1007.4005.

[49] S. Fleming, A. H. Hoang, S. Mantry, and I. W. Stewart, Phys.Rev. **D77**, 074010 (2008), hep-ph/0703207.

[50] A. H. Hoang and I. W. Stewart, Phys.Lett. **B660**, 483 (2008), arXiv:0709.3519.

[51] S. Fleming, A. H. Hoang, S. Mantry, and I. W. Stewart, Phys.Rev. **D77**, 114003 (2008), arXiv:0711.2079.

[52] V. Ahrens, T. Becher, M. Neubert, and L. L. Yang, Phys. Rev. **D79**, 033013 (2009), 0808.3008.

[53] V. Ahrens, T. Becher, M. Neubert, and L. L. Yang, Eur. Phys. J. **C62**, 333 (2009), 0809.4283.

[54] A. D. Martin, W. J. Stirling, R. S. Thorne, and G. Watt, Eur. Phys. J. **C63**, 189 (2009), 0901.0002.

[55] D. Cronin-Hennessy *et al.* [CDF Collaboration], Nucl. Instrum. Meth. **A443**, 37-50 (2000).

[56] B. Abbott *et al.* [D0 Collaboration], Phys. Rev. **D61**, 072001 (2000). [hep-ex/9906025].

[57] Heidi Schellman, private communication.

[58] Y. Li, S. Mantry, F. Petriello, [arXiv:1105.5171 [hep-ph]].

[59] R. Barlow, [physics/0401042].